LIMNOLOGY and OCEANOGRAPHY

ASLO

*Limnol. Oceanogr.* 67, 2022, S193–S207

doi: 10.1002/lno.12250

# Two temperate seagrass meadows are negligible sources of methane and nitrous oxide

**Alia N. Al-Haj** [1*], **Tyler Chidsey** [1], **Robinson W. Fulweiler** [1,2]

[1]Department of Earth & Environment, Boston University, Boston, Massachusetts
[2]Department of Biology, Boston University, Boston, Massachusetts

## *Abstract*

Seagrasses are globally important ecosystems that can help mitigate climate change by sequestering carbon (C). The net impact seagrass meadows have on the climate, however, also depends on methane ($CH_4$) and nitrous oxide ($N_2O$) fluxes. By not accounting for $CH_4$ and $N_2O$ fluxes, we may be overestimating or underestimating the true C sequestration capacity of seagrasses. Yet, few observations of seagrass $CH_4$ and $N_2O$ fluxes are available. Here, we quantified summer, dark/light $CH_4$ and $N_2O$ fluxes across the sediment–water interface from seagrass meadows (*Zostera marina*) and adjacent nonvegetated sediments in two temperate bays with different environmental characteristics. On two occasions, we also estimated system wide air-sea $CH_4$ and $N_2O$ fluxes. We found the $CH_4$ fluxes across the sediment–water interface varied between the two sites with one site emitting $CH_4$ from vegetated sediments and a net zero flux at the other site. $N_2O$ fluxes across the sediment–water interface were not different from zero regardless of seagrass presence, although when we did measure a flux, there was more often a net uptake of $N_2O$. We estimated that both systems were small net sources of $CH_4$ and $N_2O$ to the atmosphere; however, the sediments are not likely the source of $CH_4$ and $N_2O$ emitted to the atmosphere in the systems. Although the diffusive fluxes measured here are lower than those reported in the literature, they are consistent with our current understanding of seagrass sediments being variable sources of $CH_4$ and potentially a negligible source or sink of $N_2O$.

Vegetated marine ecosystems help mitigate climate change through long-term carbon (C) storage (McLeod et al. 2011; Lovelock and Duarte 2019). Chief among these "blue carbon" systems are seagrass meadows which store > 10 times more C per unit area than temperate forests (McLeod et al. 2011). To date, most research on C sequestration in seagrass ecosystems has focused on carbon dioxide ($CO_2$) uptake often ignoring two other greenhouse gases (GHGs)—methane ($CH_4$) and nitrous oxide ($N_2O$) (McLeod et al. 2011; Fourqurean et al. 2012; Tokoro et al. 2014). $CH_4$ and $N_2O$ are important because they have a sustained flux global warming potential (SGWP) 96 and 250 times that of $CO_2$, respectively, on a 20-yr time scale (Neubauer and Megonigal 2015). By neglecting $CH_4$ and $N_2O$, we are potentially miscalculating C budgets for seagrass ecosystems.

Seagrass meadows are likely "hot spots" for both the production and consumption of $CH_4$ and $N_2O$. On the one hand, the high sediment organic matter content and low/no sediment oxygen concentrations are ideal conditions for $CH_4$ and $N_2O$ formation (Murray et al. 2015; Al-Haj and Fulweiler 2020; Rosentreter et al. 2021*a*). For example, seagrass roots exude oxygen and C, potentially stimulating $N_2O$ production via nitrification and denitrification (Aoki and McGlathery 2018). Being coastal systems, seagrasses are also often exposed to high inorganic nitrogen loading which can stimulate $N_2O$ production (Orth et al. 2006; Murray et al. 2015). In addition, the shallow water column in seagrass meadows can allow $CH_4$ and $N_2O$ to quickly escape to the atmosphere before being oxidized or reduced (Gao et al. 2013; Egger et al. 2016). Finally, the seagrass plants themselves may facilitate $CH_4$ and $N_2O$ transport from the sediment to the atmosphere (Kim et al. 1999; Jørgensen et al. 2012; Jeffrey et al. 2019). On the other hand, an oxic water column and the oxygenated seagrass rhizosphere provide an opportunity for $CH_4$ and $N_2O$ uptake from the atmosphere (Deborde et al. 2010; Reading et al. 2017). For example, $CH_4$-oxidizing bacteria in the water

*Correspondence: aalhaj@bu.edu



Additional Supporting Information may be found in the online version of this article.

**Author Contribution Statement:** A.N.A. and R.W.F. both contributed equally to the study's conception and drafting the manuscript. A.N.A. led fieldwork and completed sample processing and data analysis with the help of T.J.C. All authors approve the final submitted manuscript.

**Special Issue:** Carbon sequestration in Aquatic Ecosystems. *Edited by: Isaac R. Santos, Vanessa Hatje, Oscar Serrano, David Bastviken, Dorte Krause-Jensen and Deputy Editor Julia C. Mullarney*

column and seagrass rhizosphere and anaerobic $CH_4$-oxidizing archaea in the rhizosphere can take up more $CH_4$ than is being produced in some ecosystems (Gerard and Chanton 1993; Schorn et al. 2022). $N_2O$ consumption can occur via denitrification when other sources of dissolved inorganic nitrogen (DIN) are low (Murray et al. 2015). Despite the potential for these ecosystems to be important sources or sinks of greenhouse gases, there is a paucity of data on $CH_4$ and $N_2O$ fluxes from seagrass meadows.

Filling this knowledge gap is important because increasingly, seagrass ecosystems are valued in terms of their capacity to mitigate climate change through "blue carbon" sequestration (Needelman et al. 2018; Macreadie et al. 2019). Yet, depending on the sum and direction of $CO_2$, $CH_4$, and $N_2O$ fluxes, a seagrass ecosystem may have a positive (warming) or negative (cooling) radiative balance. Some studies report $CH_4$ and $N_2O$ emissions from seagrass ecosystems which reduce or partially offset, their "blue carbon" benefit (Garcias-Bonet and Duarte 2017; Rosentreter et al. 2018). Here, we use "offset" to mean a reduction of $CO_2$ equivalent ($CO_{2eq}$) C sequestration. For example, if $CO_{2eq}$ emissions of $CH_4$ and $N_2O$ are greater than the C sequestered, the system will have net $CO_{2eq}$ emission, which will offset their blue carbon benefit and result in a positive radiative forcing (Rosentreter et al. 2021*a*). Currently, other vegetated coastal ecosystems (i.e., mangrove ecosystems) are included in several countries' Nationally Determined Contributions, and C trading markets are being established around their restoration and maintenance (Zeng et al. 2021). However, there is not enough information on $CH_4$ and $N_2O$ emissions from seagrass ecosystems to include seagrasses in these frameworks.

It is within this context that we quantified $CH_4$ and $N_2O$ fluxes across the sediment–water interface in *Zostera marina* (eelgrass) meadows in two coastal lagoons with different environmental characteristics. We also estimated system-wide air–sea fluxes of $CH_4$ and $N_2O$ from each lagoon. In addition, we measured a suite of environmental parameters that could help explain $CH_4$ and $N_2O$ fluxes from each system. We anticipated the lagoons would be sources of $CH_4$ and $N_2O$ to the atmosphere. More specifically, we hypothesized that fluxes of $CH_4$ and $N_2O$ across the sediment–water interface would be higher from vegetated sediments when compared to bare sediments, that organic matter content would be the primary driver of sediment methane emissions from these systems, and that water column DIN concentration would drive sediment $N_2O$ fluxes.

## Methods

### Site descriptions

This study was conducted in the U.S. National Park Service Cape Cod National Seashore in East Harbor (42°3′24.42″N, 70°7′10.84″W) in Truro, Massachusetts and Pleasant Bay (41°42′33.98″N, 69°57′43.96″W) in Chatham, MA (Permit # CACO-2018-SCI-0001) (Fig. 1) between July and September 2018 ($n = 1$ sampling event per site) and 2019 ($n = 2$ sampling events per site). All sampling occurred in *Zostera marina* (eelgrass)-dominated sediments and nearby (>2 m separation) nonvegetated sediments.

East Harbor is a 2.9-$km^2$ back-barrier lagoon that was cut-off from tidal flow from 1869 until 2002. In 2002, tidal flow was partially restored to East Harbor through a 200-m long, 2.2-m diameter culvert (Portnoy et al. 2006). *Z. marina* is present near the opening of the culvert (Portnoy et al. 2006) at about 1 m depth. There are currently no published estimates of *Z. marina* areal coverage in East Harbor. The lagoon has an average depth of 1 m with a tidal range of <0.5 m. Salinity in the lagoon ranges from 12 to 32 ppt and temperature ranges from ~10 °C to ~30 °C during the summer months (Portnoy et al. 2006). Water residence time in the lagoon is 133 d (Watts et al. 2011).

Pleasant Bay is a 31.7-$km^2$ coastal lagoon connected to the Atlantic Ocean by two tidal inlets. It has a tidal range of 1.4–1.6 m and an average depth of 2.0 m (Howes et al. 2006; Borrelli 2009). Salinity ranges from 29 to 31 ppt while summer water temperatures range from 12 °C to 25 °C (Legare et al. 2020). Pleasant Bay contains approximately 7.3 $km^2$ of *Z. marina* (Howes et al. 2006). Although there are natural gas deposits in Pleasant Bay, they are limited to the deeper parts of the Bay away from the shallow <2.0 m depth seagrass ecosystems where we sampled (Borrelli et al. 2020).

### Greenhouse gas fluxes across the sediment–water interface

To compare fluxes of $CH_4$ and $N_2O$ across the sediment–water interface between sites, we measured fluxes in representative stands of vegetation ($n = 3$) and in nonvegetated ($n = 3$) sediments using static chambers (collar: 20 cm diameter, 5 cm depth; plexiglass cylinder 20 cm diameter, 31.1 cm height) (Emery and Fulweiler 2014). Chambers (full description in Supporting Information Section S1; Figs. S1, S2) were covered with jackets of opaque fabric for dark incubations and the jackets were removed for light incubations. Sampling locations were chosen haphazardly but were separated by a minimum of ~ 2 m. Due to logistical constraints, nonvegetated and vegetated sediments were not sampled on the same day but were sampled on consecutive days.

We sampled the chambers immediately after sealing and at four additional time points over 80–160 min for a dark incubation with the jacket on the chamber to allow $O_2$ concentrations within the chamber to drop by at least 2 mg $L^{-1}$. We then began the light incubation by removing the jacket and sampling immediately and again at four additional time points over an additional 80–160 min. We collected duplicate water samples for $CH_4$ and $N_2O$ concentration in 12-mL exetainer vials (Labco Exetainers®). Vials were filled from the bottom up and were allowed to overflow three times before being preserved with 25 $\mu$L of saturated zinc chloride (ZnCl) solution (Ray et al. 2019). Vials were capped and stored underwater at 20°C until analysis.

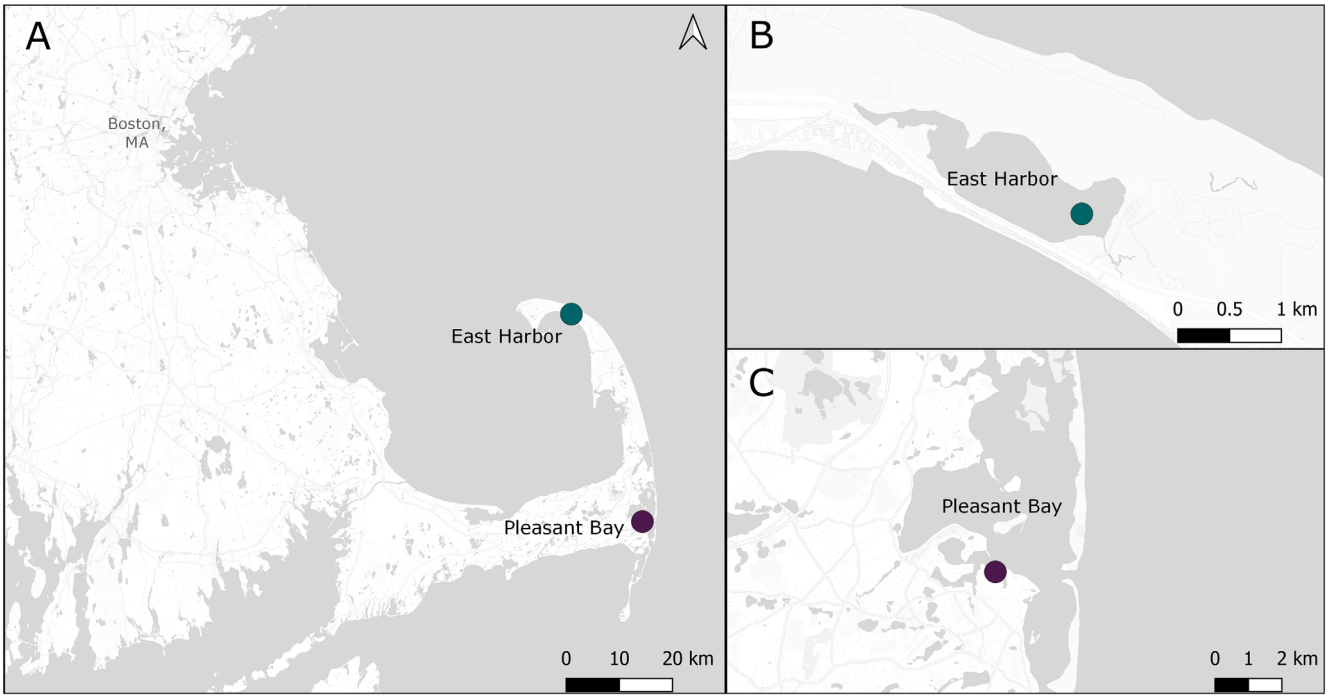


**Fig. 1.** Map of sampling locations on Cape Cod, Massachusetts, USA. (**A**) Map of Southeastern Massachusetts, USA with East Harbor (green) and Pleasant Bay (purple) highlighted by colored circles. (**B**) Map of East Harbor with sampling location depicted by green circle. (**C**) Map of Pleasant Bay with sampling location depicted by purple circle.

We measured dissolved oxygen (DO) concentration, salinity, and temperature of the chamber water at each time point using a Hach LDO101 DO sensor and a Hach CDC401 conductivity sensor. HOBO Pendant(R) light and temperature loggers recorded at one-minute intervals in each chamber for the duration of the incubation. We also collected initial and final dissolved nutrient (dissolved inorganic phosphorous [DIP], ammonium [$NH_4^+$], nitrite [$NO_2^-$], and nitrate [$NO_3^-$]) samples. Water samples were filtered in the field using a GFF filter (0.7 $\mu$m pore size) and polypropylene syringe and were stored in an acid-washed, deionized water leached polypropylene bottle at the beginning of the dark incubation, between the dark and light incubations, and at the end of the light incubation. Nutrient samples were stored on ice in the field and then at −20°C until analysis.

After each incubation was completed, we counted and collected *Z. marina* biomass from within each collar. Before removing the collar from vegetated and nonvegetated sediments, cut-off 60-cc syringes were used to collect surface (0–4 cm) sediment. Sediment subcores were sectioned into 1 cm increments for %C, %N, and C:N. Sections were stored on ice in the field and at −20 °C until analysis.

### Diffusive greenhouse gas fluxes across the air–sea interface

We estimated diffusive air–sea $CH_4$ and $N_2O$ fluxes from East Harbor and Pleasant Bay on two occasions each during Julyto September 2019 using the discreet sampling method (Rhee et al. 2009). Briefly, we collected duplicate water samples (in 12-mL Labco Exetainers) from the water surface and duplicate air samples from ~1 m above the water surface every hour for 6–9 h between the hours of 9:00 EST and 17:00 EST. We collected 25 mL of air with a 60-cc polypropylene syringe for each gas sample and transferred the gas into an evacuated 12-mL exetainer through a 25-G needle. Water samples were stored and preserved in the same manner as sediment–water interface flux samples, and gas samples were stored at 4 °C until analysis. Although we collected these samples within the *Z. marina* meadows, we consider them to be representative of the diffusive air–sea flux for the entire system (i.e., influenced by seagrass and bare sediment) as these are open system measurements with tidal water transport.

### Sample analysis and flux determination

#### *Greenhouse gas sample analysis*

We quantified $CH_4$ and $N_2O$ concentrations in each water sample using a headspace equilibration technique with the headspace then analyzed on a GC-2014 gas chromatograph (Shimadzu) (Ray et al. 2019) (full description in Supporting Information Section S2).

We determined concentrations of $CH_4$ and $N_2O$ by comparing sample peak area to a standard curve calculated from the peak area of six different concentrations of an externally mixed standard (Airgas; Supporting Information Section S3). The amount of gas in the headspace was calculated using the

ideal gas law, the amount of dissolved gas was determined using Henry's law, and the solubility coefficients determined by the equations and constants for $CH_4$ (Wiesenburg and Guinasso 1979) and $N_2O$ (Weiss and Price 1980).

### *Equilibrium solubility and % saturation*

Equilibrium solubilities for $CH_4$ and $N_2O$ surface water samples were determined using methods from Wiesenburg and Guinasso (1979) and Weiss and Price (1980), respectively (Supporting Information Section S4).

Percent saturation (% sat) of each gas in the water column was calculated as the ratio of observed concentration ($C_{obs}$) to equilibrium concentration ($C_{eq}$) (Tseng et al. 2016):

$$\%\text{sat} = \left(C_{obs}/C_{eq}\right) * 100. \quad (1)$$

### *Flux calculations*

Fluxes across the sediment–water interface were determined as the linear change in concentration of $CH_4$ or $N_2O$ over time accounting for chamber volume and area. For a flux to be considered significant, $R^2 \geq 0.65$ and $p \leq 0.10$. If these criteria were not met, we considered that no flux was observed, and a value of 0 was assigned (Ray et al. 2019).

Diffusive air–sea fluxes were estimated using the disequilibrium flux equation (Liss and Merlivat 1986; Weber et al. 2019). The disequilibrium flux was calculated as the change in concentration between surface water concentration and atmospheric equilibrium concentration:

$$F = k\left[C_w - \left(S * p_{moist}\right)\right], \quad (2)$$

where $F$ is the flux ($\mu$mol m$^{-2}$ h$^{-1}$), $k$ is the gas transfer velocity (cm hr$^{-1}$), $C_w$ is the concentration of the gas in water ($\mu$mol L$^{-1}$), $S$ is the solubility of the gas at the temperature and salinity of the measurement ($\mu$mol L$^{-1}$), and $p_{moist}$ is the partial pressure of the gas in moist air (mol of gas/mol dry air) (Wiesenburg and Guinasso 1979; Weiss and Price 1980; Weber et al. 2019). Because we do not have system specific gas transfer velocity equations, we used the average gas transfer velocity calculated from five equations commonly used in coastal ecosystems (Supporting Information Table S2). Gas transfer velocity ($k$) is commonly calculated as a function of wind speed (Clark et al. 1995; Carini et al. 1996; Jiang et al. 2008; Wanninkhof 2014) with others adding terms for current velocity and depth in shallow coastal systems (Borges et al. 2004; Rosentreter et al. 2017). We did not measure water velocity in our basins, so we only used gas transfer velocity calculations that are a function of wind speed. Average daily wind speed during the sampling period was obtained from the nearest NOAA meteorological station to each site (Pleasant Bay: Chatham Airport USW00094624, 3.5 km from site; East Harbor: Sta. 44018, 17 km from site). Wind speeds were recalculated to a height of 10 m ($U_{10}$) using the equation provided in Amorocho and DeVries (1980):

$$U_z = U_{10}\left[1 - \frac{(C_{10})^{1/2}}{\kappa}\ln\left(\frac{10}{z}\right)\right], \quad (3)$$

where $C_{10}$ is the surface drag coefficient for wind at 10 m (0.0013), $\kappa$ is the Van Karman constant (0.41), and $z$ is the height the wind speed was measured at above the water

**Table 1.** Overview of site characteristics for vegetated and non-vegetated sediments of East Harbor and Pleasant Bay. Mean (± SE) seagrass density, LAI, and NPI (% leaf N/area normalized leaf mass), surface (top ~ 10 cm) water column salinity, and nutrient concentrations ($NH_4^+$, $NO_2^-$, $NO_3^- + NO_2^-$ : $NO_x$, DIN, and DIP), and sediment surface (top 0–1 cm depth) %N, %C, and C : N from one sampling date for each site during summer 2018 and two sampling dates for each site during summer 2019. Superscripts of differing letters indicate statistically different (least square means, $p < 0.05$) values between sites and vegetated and nonvegetated sediments.

| | | East Harbor | | Pleasant Bay | |
|---|---|---|---|---|---|
| | | Eelgrass | Non-vegetated | Eelgrass | Non-vegetated |
| Seagrass | Density (shoots m$^{-2}$) | 305.9 (± 34.9)$^a$ | 0.0 (± 0.0)$^b$ | 410.3 (± 48.2)$^a$ | 0.0 (± 0.0)$^b$ |
| | LAI (m$^2$ m$^{-2}$) | 0.0084 (± 0.0013)$^a$ | 0.0 (± 0.0)$^b$ | 0.0072 (± 0.0014)$^a$ | 0.0 (± 0.0)$^b$ |
| | NPI (%N/mg dry leaf mass cm$^{-2}$) | 0.65 (± 0.23)$^a$ | — | 1.15 (± 0.27)$^a$ | — |
| Water column | Salinity (ppt) | 25.6 (± 0.5)$^a$ | 25.9 (± 0.4)$^a$ | 32.4 (± 0.1)$^b$ | 32.6 (± 0.1)$^b$ |
| | $NH_4^+$ ($\mu$M) | 0.74 (± 0.18)$^a$ | 0.99 (± 0.14)$^a$ | 3.52 (± 0.73)$^b$ | 2.02 (± 0.19)$^{ab}$ |
| | $NO_2^-$ ($\mu$M) | 0.04 (± 0.005)$^a$ | 0.04 (± 0.005)$^a$ | 0.04 (± 0.007)$^a$ | 0.05 (± 0.005)$^a$ |
| | $NO_x$ ($\mu$M) | 0.13 (± 0.031)$^{ac}$ | 0.11 (± 0.011)$^a$ | 0.21 (± 0.033)$^{bc}$ | 0.24 (± 0.013)$^b$ |
| | DIN ($\mu$M) | 0.90 (± 0.211)$^a$ | 1.01 (± 0.158)$^a$ | 3.77 (± 0.754)$^b$ | 2.05 (± 0.250)$^a$ |
| | DIP ($\mu$M) | 0.38 (± 0.036)$^a$ | 0.45 (± 0.023)$^a$ | 1.07 (± 0.137)$^b$ | 0.76 (± 0.029)$^c$ |
| Sediment | N (%) | 0.039 (± 0.005)$^a$ | 0.043 (± 0.003)$^a$ | 0.092 (± 0.009)$^b$ | 0.036 (± 0.005)$^a$ |
| | C (%) | 0.448 (± 0.071)$^{ac}$ | 0.728 (± 0.081)$^{ab}$ | 0.902 (± 0.118)$^b$ | 0.373 (± 0.031)$^c$ |
| | C : N | 13.28 (± 0.59)$^a$ | 20.18 (± 2.30)$^b$ | 11.14 (± 0.60)$^a$ | 13.37 (± 1.27)$^a$ |

surface (m) (Rosentreter et al. 2017). We normalized $k$ to a Schmidt number (Sc) as a function of temperature and salinity for each gas using the equations provided in Wanninkhof (2014).

$$k = 0.251 < U^2 > \left(\frac{\mathrm{Sc}}{X}\right)^{-0.5}, \quad (4)$$

where $U$ is the wind speed, Sc is the Schmidt number calculated as a function of temperature and salinity for each gas, $X$ is the Schmidt number of each gas in seawater at 20°C as reported in Wanninkhof (2014), and −0.5 is the Schmidt exponent.

Daily sediment–water interface fluxes were calculated by multiplying dark and light fluxes by 12 h $d^{-1}$. Then the sum of 12 h dark and light fluxes were calculated. Daily air–sea interface fluxes were calculated by multiplying hourly air–sea fluxes by 24 h $d^{-1}$.

### *Nutrient analyses*

Dissolved inorganic nutrient (DIP, $NH_4^+$, $NO_2^-$, and $NO_3^-$) concentrations were determined via digital colorimetry on a SEAL Auto-Analyzer 3 using standard techniques (Strickland and Parsons 1968) with method detection limits of 0.010, 0.080, 0.006, and 0.013 $\mu$M, respectively.

### *Sediment characteristics*

Sediment subsections were homogenized and dried at 60°C for at least 48 h before being ground. %C and %N content per gram of dried sediment was determined on an Elemental Combustion System 4010 (Costech Analytical Technologies) elemental analyzer.

### *Plant morphometrics and biogeochemistry*

To characterize each seagrass meadow, we determined seagrass density, biomass, leaf area index (LAI), and nutrient pollution indicator (NPI). Seagrass density at each sampling location was determined by counting the number of ramets within each chamber base area. Biomass was collected by trimming the seagrass at the sediment surface at the end of the incubation. Shoots were stored at 3°C until leaves were separated from sheaths and leaf length and width were measured. Biomass was determined by drying the leaves and collected sheaths at 60°C for a minimum of 48 h, weighing, and normalizing over chamber base area.

LAI was calculated using the following equation:

$$\mathrm{LAI} = l \times w, \quad (5)$$

where $l$ is the length of the seagrass blade and $w$ is the width of the seagrass blade. NPI was calculated as the ratio of leaf %N to area normalized leaf mass where leaf %N was determined via elemental analysis (Lee et al. 2004).

**Table 2.** Concentrations (mean ± SE) of methane ($CH_4$) and nitrous oxide ($N_2O$) in air and water and percent saturation (% Sat) in surface water in East Harbor and Pleasant Bay during summer 2019. Superscripts of differing letters indicate statistically different (least square means, $p < 0.05$) values between sites and dates.

| | | Air | | | | Water | | | |
|---|---|---|---|---|---|---|---|---|---|
| | | $CH_4$ | | $N_2O$ | | $CH_4$ | | $N_2O$ | |
| Site | Date | ppm | nmol $L^{-1}$ | ppb | nmol$L^{-1}$ | nmol $L^{-1}$ | %Sat | nmol $L^{-1}$ | %Sat |
| East Harbor | 16 Jul 2019 | 2.05 ± 0.05 | 81.15 ± 1.63$^{a}$ | 280.68 ± 1.41 | 11.63 ± 0.06$^{a}$ | 98.77 ± 10.52$^{a}$ | 4165.15 ± 464.57$^{a}$ | 11.76 ± 0.31$^{a}$ | 206.30 ± 5.48$^{a}$ |
| | 20 Aug 2019 | 1.82 ± 0.03 | 74.66 ± 1.27$^{ab}$ | 278.21 ± 1.84 | 11.53 ± 0.08$^{a}$ | 30.44 ± 1.20$^{b}$ | 1414.80 ± 111.16$^{b}$ | 9.13 ± 0.50$^{b}$ | 158.74 ± 9.06$^{bc}$ |
| | 21 Aug 2019 | 1.78 ± 0.10 | 72.90 ± 4.25$^{ab}$ | 268.78 ± 15.59 | 11.14 ± 0.65$^{a}$ | 29.16 ± 1.21$^{b}$ | 1405.63 ± 127.78$^{b}$ | 10.21 ± 0.16$^{b}$ | 193.91 ± 16.66$^{ab}$ |
| Pleasant Bay | 06 Aug 2019 | 1.88 ± 0.06 | 77.47 ± 2.61$^{ab}$ | 268.61 ± 1.91 | 11.13 ± 0.08$^{a}$ | 110.97 ± 11.04$^{a}$ | 4872.25 ± 576.80$^{a}$ | 12.30 ± 0.24$^{a}$ | 203.78 ± 5.14$^{a}$ |
| | 07 Aug 2019 | 1.85 ± 0.04 | 76.34 ± 1.78$^{ab}$ | 267.54 ± 2.42 | 11.09 ± 0.10$^{a}$ | 100.84 ± 3.64$^{a}$ | 4453.45 ± 188.03$^{a}$ | 11.74 ± 0.38$^{a}$ | 194.22 ± 4.80$^{ab}$ |
| | 04 Sep 2019 | 1.73 ± 0.01 | 72.11 ± 0.54$^{b}$ | 282.10 ± 1.53 | 11.74 ± 0.08$^{a}$ | 81.50 ± 3.94$^{a}$ | 3713.76 ± 170.28$^{a}$ | 9.47 ± 0.15$^{b}$ | 141.19 ± 2.33$^{c}$ |
| | 05 Sep 2019 | 1.67 ± 0.03 | 69.79 ± 1.15$^{b}$ | 269.68 ± 4.72 | 11.17 ± 0.20$^{a}$ | 86.46 ± 4.59$^{a}$ | 3959.68 ± 217.88$^{a}$ | 8.96 ± 0.14$^{b}$ | 132.82 ± 2.51$^{c}$ |

### Statistical analyses

All statistical analyses were performed using R version 4.0.3. Results of statistical tests were considered significant when $p < 0.05$. We tested whether $CH_4$ and $N_2O$ fluxes across the sediment–water interface were different between seagrass sites and bare sediments using a mixed model approach. Because the gas flux data are zero-inflated, we modeled our zeros using a zero-adjusted gamma modification to the classic hurdle model (Zuur and Ieno 2016). Briefly, we performed a Gamma log-link generalized linear model (GLM) on the nonzero data using location, vegetation presence, light treatment, month, and year as fixed effects. We then performed a Bernoulli GLM to identify the chance that a data point is not zero. We subsequently combined the models, calculated Pearson residuals, and combined modeled zeros with the nonzero flux data into one data frame. We then determined the distribution of these data using the *fitdistrplus* package (Delignette-Muller and Dutang 2015). We found that $CH_4$ and $N_2O$ data best fit a normal distribution.

We tested whether mean sediment–water interface and air–sea fluxes of $CH_4$ and $N_2O$ from each site, vegetation treatment, and light treatment were significantly different from zero using a one-sample *t*-test.

We determined if predictor variables were correlated (Supporting Information Table S3) and chose noncorrelated predictor variables to use in the model. We then generated multiple generalized linear models using the *lme4* package (Bates et al. 2015; Ray et al. 2019). The presence or absence of seagrass, location, and light treatment were treated as fixed effects in the models along with other noncorrelated predictor variables (e.g., $O_2$ flux, salinity, LAI; Supporting Information Tables S4–S6). A total of 125 models were constructed for fluxes of each gas. We used Akaike information criterion (AIC) to select the best models (Bozdogan 1987) and then compared the top two models using likelihood ratio tests with the *lrtest* function in the *lmtest* package (Hothorn et al. 2020; Supporitng Information Table S4). When the top two models were not significantly different, we chose to use the simpler model (Supporting Information Tables S5, S6).

Differences between sites, vegetation treatment, and light treatment were determined using a least square means test on sediment and water column characteristics.

## Results

### Site characterization

Water column salinity, $NH_4^+$, $NO_x$, DIN, and DIP concentrations differed significantly between sites with higher salinity and nutrient concentrations in Pleasant Bay (Table 1). However, there was no statistical difference among seagrass density, LAI, or NPI between sites (Table 1). Sediment characteristics differed between sites and with eelgrass presence, though not in a consistent pattern (Table 1).

### Greenhouse gas concentrations and fluxes

Recent work on $CH_4$ concentrations in Boston (approximately 90 km west of the study site) reported peak $CH_4$ concentrations of 2.6 ppm (Sargent et al. 2021). 20% of East Harbor atmospheric gas samples and 2% of Pleasant Bay atmospheric gas samples had $CH_4$ concentrations greater than this peak concentration. Although the data we report here met all QA/QC criteria and we have no reason to suspect that the concentrations are incorrect, we decided to take a conservative approach and remove values exceeding 2.6 ppm from downstream analysis for the air–sea flux calculation. We do, however, include the full dataset analysis in Supporting Information Table S1, and all data are available via Figshare (doi: 10.6084/m9.figshare.20079470).

Atmospheric $CH_4$ concentrations were highest on 16 July 2019 in East Harbor and lowest during September 2019 sampling dates in Pleasant Bay ($F_{6,36} = 3.21$, $R^2 = 0.24$, $p = 0.01$), while atmospheric $N_2O$ concentrations were similar across sites and dates ($F_{6,37} = 1.09$, $R^2 = 0.01$, $p = 0.39$) (Table 2).

**Table 3.** Fluxes (mean ± SE) of methane ($CH_4$) and nitrous oxide ($N_2O$) from eelgrass vegetated and non-vegetated sediments in East Harbor and Pleasant Bay. Fluxes across the sediment–water interface are the mean of measurements from summer 2018 and 2019. Air–sea fluxes are from summer 2019. Letters indicate statistically significant (least square means, $p < 0.05$) differences between sites, vegetated and non-vegetated sediments, and light treatment. Italicized fluxes are not significantly different from zero.

| | | | Sediment–water interface flux ($\mu$mol m$^{-2}$ h$^{-1}$) | | Whole system air–sea flux ($\mu$mol m$^{-2}$ h$^{-1}$) | |
|---|---|---|---|---|---|---|
| Location | Vegetation | Light | $CH_4$ | $N_2O$ | $CH_4$ | $N_2O$ |
| East Harbor | Eelgrass | Light | *0.75 (± 0.44)*$^{ab}$ | *−0.02 (± 0.02)*$^{a}$ | 4.48 (± 0.59)$^{a}$ | 0.40 (± 0.03)$^{a}$ |
| | | Dark | *0.55 (± 0.50)*$^{ab}$ | *−0.02 (± 0.01)*$^{a}$ | | |
| | Non-vegetated | Light | *0.91 (± 0.44)*$^{ab}$ | *−0.01 (± 0.01)*$^{a}$ | | |
| | | Dark | *0.31 (± 0.16)*$^{ab}$ | *−0.00 (± 0.00)*$^{a}$ | | |
| Pleasant Bay | Eelgrass | Light | 2.21 (± 0.92)$^{bc}$ | *−0.02 (± 0.07)*$^{a}$ | 4.74 (± 0.20)$^{a}$ | 0.22 (± 0.02)$^{b}$ |
| | | Dark | 3.90 (± 0.82)$^{c}$ | *0.04 (± 0.05)*$^{a}$ | | |
| | Non-vegetated | Light | *−0.17 (± 0.31)*$^{a}$ | *0.00 (± 0.00)*$^{a}$ | | |
| | | Dark | *−0.28 (± 0.18)*$^{a}$ | *−0.03 (± 0.02)*$^{a}$ | | |

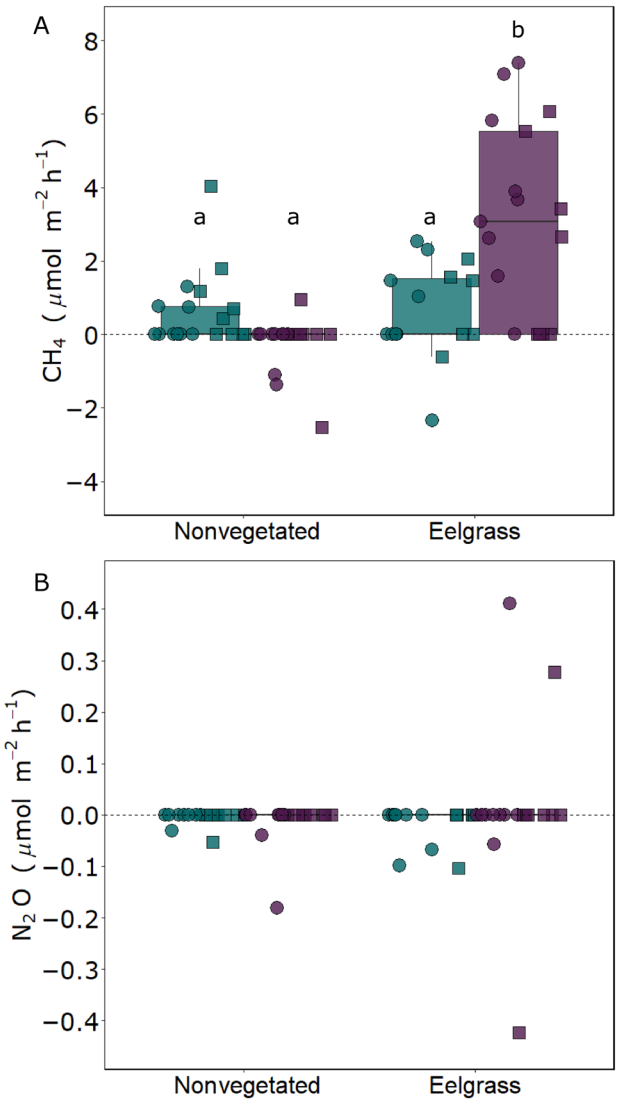


**Fig. 2.** Fluxes of methane ($CH_4$) (**A**) and nitrous oxide ($N_2O$) across the sediment–water interface (**B**) from eelgrass vegetated and non-vegetated sediments in East Harbor (green) and Pleasant Bay (purple) over light (square) and dark (circle) incubations. Positive fluxes indicate emission into the water column while negative fluxes indicate uptake by the sediment. Lower-case letters indicate significant differences ($p \leq 0.05$) across both vegetation treatment and site following least-square means test. There were no significant differences across site and vegetation treatment for $N_2O$ fluxes. Individual points represent flux measurements.

Surface water $CH_4$ and $N_2O$ concentrations were supersaturated in both basins but were variable across sites and dates with significantly lower $CH_4$ concentrations in East Harbor during late August 2019 ($F_{6,37} = 16.03$, $R^2 = 0.67$, $p < 0.0001$) and significantly lower concentrations of $N_2O$ in both basins during late August and early September ($F_{6,37} = 18.51$, $R^2 = 0.71$, $p < 0.0001$; Table 2).

Fluxes of $CH_4$ and $N_2O$ across the sediment–water interface were highly variable and zero-inflated. $CH_4$ fluxes ranged from −2.52 to 7.38 $\mu$mol $m^{-2}$ $h^{-1}$ with 51% of the $CH_4$ flux measurements exhibiting a net zero flux. $N_2O$ fluxes ranged from −0.42 to 0.41 $\mu$mol $m^{-2}$ $h^{-1}$ with 84% of the $N_2O$ flux measurements exhibiting a net zero flux.

On average, sediment–water interface fluxes of $CH_4$ and $N_2O$ were not significantly different from zero except for vegetated sediments in Pleasant Bay which were the only sediments to exhibit mean fluxes that were significantly different from zero (light: $t_7 = 2.41$, $p = 0.047$; dark: $t_8 = 4.73$, $p < 0.005$) (Table 3; Supporting Information Table S7). $CH_4$ was emitted into the water column from vegetated sediments in Pleasant Bay (Fig. 2A). There was no difference in $CH_4$ flux across the sediment–water interface for light and dark treatments within Pleasant Bay or East Harbor ($t_{33} = 1.02$, $p = 0.32$; $t_{31} = -1.03$, $p = 0.31$, respectively) (Supporting Information Table S9) nor between the two sites ($t_{66} = -1.62$, $p = 0.11$) (Table 3; Supporting Information Table S11).

Estimated diffusive air-sea fluxes of $CH_4$ and $N_2O$ were significantly different from zero although relatively low in both systems. Diffusive air–sea flux of $CH_4$ did not differ between locations with both sites acting as a source of $CH_4$ to the atmosphere ($F_{1,41} = 0.42$, $p = 0.52$) (Table 3). Estimated diffusive air–sea fluxes of $N_2O$ were higher in East Harbor than in Pleasant Bay with both systems acting as

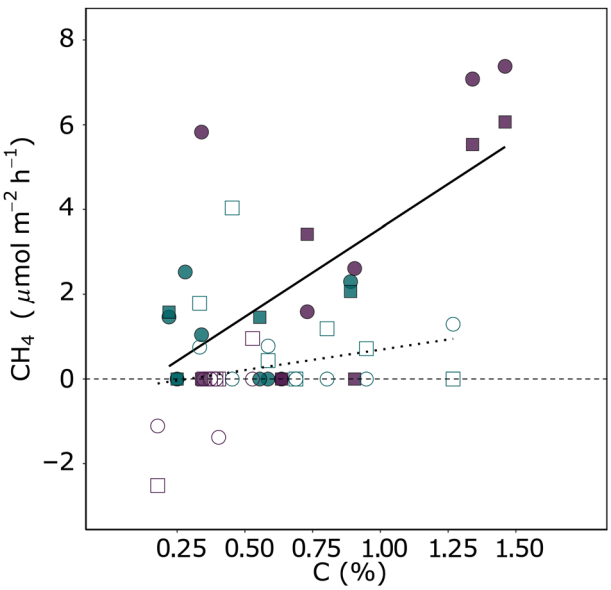


**Fig. 3.** Fluxes of methane ($CH_4$) across the sediment–water interface as a function of %C in the surface (top 0–1 cm) of sediment from eelgrass vegetated (filled points) and nonvegetated (open points) sediments in East Harbor (green) and Pleasant Bay (purple) over light (square) and dark (circle) incubations. Positive fluxes indicate emission into the water column while negative fluxes indicate uptake by the sediment. The solid line indicates the relationship between $CH_4$ flux and %C in vegetated sediments ($y = 4.18x - 0.63$, $R^2 = 0.45$, $p < 0.0005$). There is no relationship between $CH_4$ flux and %C in nonvegetated sediments (dotted line, $R^2 = 0.02$, $p = 0.23$).

**Table 4.** Mean fluxes of methane ($CH_4$) and nitrous oxide ($N_2O$) across the air–sea or sediment–water column (sed-wc) interface in seagrass vegetated sediments from previously published studies. Diffusive fluxes are dissolved gas fluxes while ebullitive fluxes are bubble fluxes. The bottom two rows are the mean (± SE) sediment–water column interface and air–sea fluxes. The mean sediment–water column interface and air–sea fluxes (final two rows) represent an average of the sediment–water column interface and air–sea fluxes from the previously published studies and this study.

| Site | Species | Flux type | $CH_4$ flux ($\mu$mol $m^{-2}$ $d^{-1}$) | $N_2O$ flux ($\mu$mol $m^{-2}$ $d^{-1}$) | Citation |
|---|---|---|---|---|---|
| Ria Formosa Lagoon, Portugal | *Zostera noltii* | Air–sea diffusive | 307.2 | | Bahlmann et al. (2015) |
| Chilika Lagoon, India | *Halodule-Halophila* spp. | Air–sea diffusive | 120.0 | | Banerjee et al. (2018) |
| Arcachon Lagoon, France | *Zostera marina* | Air–sea diffusive | 294.0 | | Deborde et al. (2010) |
| Chwaka Bay, Tanzania | *Thalassia hemprichii* | Air–sea diffusive | 74.7 | | Lyimo et al. (2018) |
| Red Sea, Saudi Arabia | *Halophila stipulacea* | Air–sea diffusive | 60.2 | | Burkholz et al. (2020) |
| Wallagoot, Australia | *Ruppia megacarpa* | Air–sea diffusive | 33.8 | −0.9 | Camillini (2020) |
| East Harbor, Massachusetts | *Zostera marina* | Air–sea diffusive | 107.5 | 9.6 | This study |
| Pleasant Bay, Massachusetts | *Zostera marina* | Air–sea diffusive | 113.8 | 5.3 | This study |
| Awerange Bay, Indonesia | *Enhalus acoroides* | Sed–wc diffusive | 95.7 | | Alongi et al. (2008) |
| Florida, USA | *Thalassia testudinum* | Sed–wc diffusive | 135.9 | | Barber and Carlson (1993) |
| Arcachon Lagoon, France | *Zostera marina* | Sed–wc diffusive | 48.8 | | Deborde et al. (2010) |
| Red Sea, Saudi Arabia | *Halodule uninervis* | Sed–wc diffusive | 48.2 | | Garcias-Bonet and Duarte (2017) |
| Red Sea, Saudi Arabia | *Cymodocea and Halodule* spp. | Sed–wc diffusive | 401.3 | | Garcias-Bonet and Duarte (2017) |
| Red Sea, Saudi Arabia | *Enhalus acoroides* | Sed–wc diffusive | 96.2 | | Garcias-Bonet and Duarte (2017) |
| Red Sea, Saudi Arabia | *Thalassodendron ciliatum* | Sed–wc diffusive | 3.2 | | Garcias-Bonet and Duarte (2017) |
| Red Sea, Saudi Arabia | *Halophila decipiens* | Sed–wc diffusive | 1.4 | | Garcias-Bonet and Duarte (2017) |
| Red Sea, Saudi Arabia | *Thalassia hemprichii* | Sed–wc diffusive | 6.5 | | Garcias-Bonet and Duarte (2017) |
| Red Sea, Saudi Arabia | *Halophila* and *Halodule* spp. | Sed–wc diffusive | 61.0 | | Garcias-Bonet and Duarte (2017) |
| Florida, USA | *Thalassia testudinum* | Sed–wc diffusive | 44.0 | | Oremland (1975) |
| Bimini, Bahamas | *Syringodium filiforme* | Sed–wc diffusive | 5.8 | | Oremland (1975) |
| South Bay, Virginia | *Zostera marina* | Sed–wc ebullitive | 136.7 | 3.7 | Oreska et al. (2020) |
| Tomales Bay, California | *Zostera marina* | Sed–wc diffusive | 35.8 | | Sansone et al. (1998) |
| Wallis Lake (Australia) | *Halophila ovalis* | Sed–wc diffusive | 45.4 | 0.3 | Camillini (2020) |
| Wallis Lake (Australia) | *Posidonia australia* | Sed–wc diffusive | 279.3 | −0.6 | Camillini (2020) |
| Wallis Lake (Australia) | *Zostera muelleri* | Sed–wc diffusive | 46.0 | −1.2 | Camillini (2020) |
| Moreton Bay, Australia | *Zostera muelleri* | Sed–wc diffusive | 10.9 | | Moriarty et al. (1985) |
| East Harbor, Massachusetts | *Zostera marina* | Sed–wc diffusive | 0.0 | 0.0 | This study |
| Pleasant Bay, Massachusetts | *Zostera marina* | Sed–wc diffusive | 73.3 | 0.0 | This study |
| Mean (± SE) | | Air–sea | 138.9 (± 34.4) | 4.7 (± 2.5) | |
| | | Sed–wc | 78.8 (± 22.5) | 0.4 (± 0.6) | |

small sources of atmospheric $N_2O$ ($F_{1,42}$ = 27.09, $p < 0.0001$; Table 3).

### Drivers of greenhouse gas fluxes across the sediment–water interface

$CH_4$ fluxes across the sediment–water interface were best explained by presence or absence of seagrass and %C in the top 0–1 cm of sediment (Fig. 3; Supporting Information Tables S4, S5). Specifically, in vegetated sediments there was a positive relationship between $CH_4$ flux across the sediment–water interface and %C in the top 0–1 cm of sediment. There was no relationship between $CH_4$ flux across the sediment–water interface and %C in the top 0–1 cm of sediment for nonvegetated sediments. The environmental variables we measured did not explain $N_2O$ fluxes (Supporting Information Tables S4, S6).

## Discussion

### $CH_4$ and $N_2O$ fluxes across the sediment–water interface

Here, we show that $CH_4$ fluxes from *Z. marina* meadows in two temperate ecosystems were variable and that $N_2O$ fluxes,

at least when we sampled, were negligible. As we hypothesized, $CH_4$ fluxes across the sediment–water interface were higher from *Z. marina* meadows in Pleasant Bay (Fig. 2A). In contrast, there was no significant difference in $CH_4$ flux from East Harbor between seagrass and nonvegetated sediments. The results from East Harbor were different from previous studies on *Z. marina* as well as from other seagrass species where it has been consistently shown that vegetated sediments have higher $CH_4$ fluxes (Table 4).

One reason for the differences in $CH_4$ emissions between the two *Z. marina* systems studied here could be due to organic matter quantity and quality. Previous studies in wetland ecosystems have found positive correlations between organic matter content and quality and $CH_4$ emissions (mangrove: Harttung et al. 2021; Konnerup et al. 2014, freshwater: Grasset et al. 2021). For example, soil organic matter content was a strong predictor of $CH_4$ emissions across three saltmarsh to mangrove transition zones in Florida, USA (Harttung et al. 2021). Methane emission and organic matter content were also highly positively correlated ($r = 0.75$) in the restored mangrove forests of Ciénaga Grande de Santa Marta, Colombia (Konnerup et al. 2014), and for inland waters, $CH_4$ production can be predicted by organic matter content and quality (Grasset et al. 2021). Here, we found that higher sediment carbon content was positively correlated ($p < 0.0005$) with $CH_4$ flux across the sediment–water interface in vegetated sediments (Fig. 3). We also looked at the sediment C:N content, as a proxy for organic matter lability (i.e., high C:N suggests recalcitrant organic matter, low C:N suggests labile organic matter). Again, for the vegetated sediments we found that higher sediment C:N was predictive of higher $CH_4$ flux across the sediment–water interface; sediment C:N was not predictive of $CH_4$ flux across the sediment–water interface from nonvegetated sites (Fig. 3). Together these relationships suggests that less labile organic matter is driving $CH_4$ emissions in vegetated areas. Alternatively, the relationship may suggest that the abundance of organic matter associated with seagrass sediments provides enough substrate for methanogenesis to occur, leaving less labile organic material in the sediments (Trevathan-Tackett et al. 2018). Seagrasses produce many N-containing methylated compounds (Schorn et al. 2022) which could also serve as substrates for $CH_4$ production in areas with lower C:N ratios, as in Pleasant Bay. In contrast, nonvegetated sediments may not have a consistent source of labile organic material for methane production; however, methane consumption can still occur in these sediments due to the high concentrations of $CH_4$ in the water column. Regardless, data from this study and those previously published suggest that sediment C:N and/or %C may be an important predictor variable for $CH_4$ fluxes.

Substrate availability and competition for substrates for methanogenesis drive $CH_4$ source and sink dynamics in coastal ecosystems. For example, $CH_4$ fluxes in tidal marshes are driven by the competition between sulfate reducers and methanogens (Poffenbarger et al. 2011). Similar to other studies in seagrass ecosystems (Garcias-Bonet and Duarte 2017; Al-Haj and Fulweiler 2020), we found no pattern between $CH_4$ emissions and salinity, further demonstrating that the negative relationship between $CH_4$ emission and salinity observed for tidal marshes (Poffenbarger et al. 2011) does not hold in seagrass ecosystems. Although $CH_4$ fluxes in saline tidal marshes are driven by competition between sulfate-reducing bacteria and hydrogenotrophic and acetoclastic methanogens (DeLaune et al. 1983; Bartlett et al. 1987), different mechanisms must control $CH_4$ production in seagrass ecosystems. For seagrass ecosystems, methane emission may occur because there is either enough organic matter in the system to meet the demands of sulfate-reducing bacteria allowing

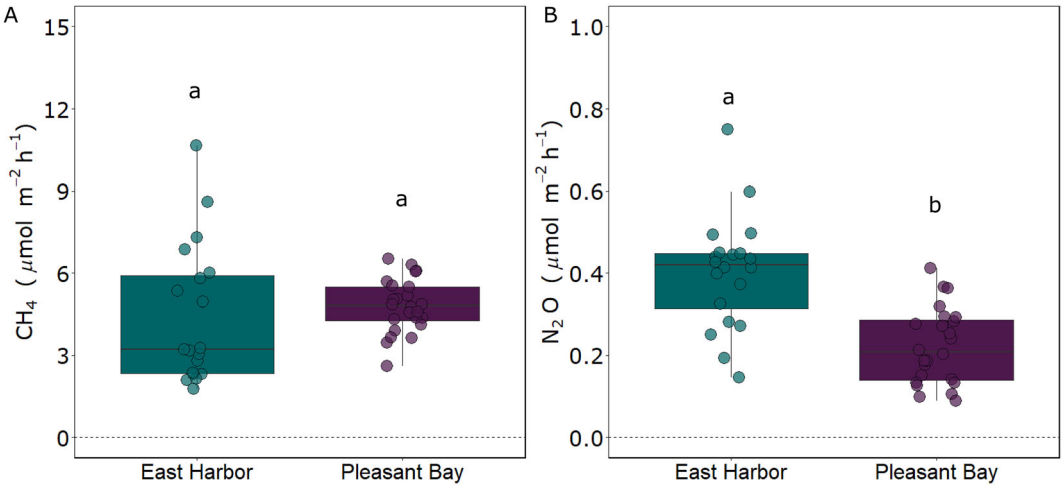


**Fig. 4.** Methane ($CH_4$) (**A**) and nitrous oxide ($N_2O$) (**B**) fluxes across the air-sea interface from East Harbor (green) and Pleasant Bay (purple). Positive fluxes indicate emission into the atmosphere. Lower-case letters indicate significant differences ($p \leq 0.05$) between sites following least-square means test. There were no significant differences between sites for $CH_4$ fluxes. Individual points represent flux measurements.

hydrogenotrophic and acetoclastic methanogens access to organic material to produce $CH_4$ or a noncompetitive form of methanogenesis (methylotrophic methanogenesis or aerobic methane production) is occurring in these systems (Reeburgh 2007). A recent study comparing methanogenic communities in trimethylamine amended *Z. marina* vegetated and nonvegetated sediments found that methane emissions increased with amendment and that there was a higher abundance of methylotrophic methanogens in vegetated sediments (Zheng et al. 2020). Recent studies from unvegetated coastal sediments also suggest methylotrophic methanogenesis dominates (Zhuang et al. 2018; Yuan et al. 2019).

We hypothesized that $N_2O$ emissions would be higher in vegetated sediments compared to nonvegetated sediments. However, we found no difference in $N_2O$ emissions between eelgrass vegetated and nonvegetated sediments at either site, and the average net sediment–water interface $N_2O$ fluxes did not differ from zero. The results differ from other studies on *Z. marina*, which found vegetated areas either emit or take up $N_2O$ (Camillini 2020; Oreska et al. 2020) (Table 4).

One reason for the difference between Oreska et al. (2020) and our study could be due to differences in methods. Although we and Camillini (2020) measured diffusive $N_2O$ flux across the sediment–water interface, Oreska et al. (2020) measured ebullitive flux. In other systems (e.g., streams, reservoirs, peatlands), ebullitive fluxes of $N_2O$ are lower than diffusive fluxes (Sturm et al. 2014; Descloux et al. 2017). Oreska et al. (2020); however, report ebullitive fluxes more than 10 times higher than the diffusive fluxes we observed and those reported in Camillini (2020). Part of the ebullitive flux Oreska et al. (2020) detected may have been due to flux through the eelgrass itself. Plant-mediated fluxes of $N_2O$ have been shown to be important in other vegetated systems. For example, in rice paddy ecosystems, up to 80% of $N_2O$ emissions are plant mediated (Yu et al. 1997). Because *Z. marina* is predominantly submerged, plant-mediated flux of gases would take the form of bubbles and become part of the ebullitive flux (Long et al. 2020), suggesting that plant-mediated flux may be an important pathway for $N_2O$ emission in seagrass ecosystems and may have the potential to change systems from a sink to a source of $N_2O$.

Because the $N_2O$ fluxes across the sediment–water interface were so low in our system, we were unable to determine what drives these fluxes. Vegetation presence was not present in the best sediment–water interface $N_2O$ model (Supporting Information Table S3). Other studies found that vegetation presence and vegetation type significantly impacted $N_2O$ emissions (Murray et al. 2015; Gao et al. 2019; Yang et al. 2020). Other common drivers of $N_2O$ emission (i.e., $NH_4^+$, $O_2$ concentrations, and temperature) were present in the best model, however, this model was not statistically significant (Supporting Information Table S2). There is no other evidence from seagrass ecosystems that there is a pattern between DIN or $O_2$ concentrations and $N_2O$ flux, unlike in mangrove, salt marsh, and nonvegetated estuarine systems (Murray et al. 2015). Another seagrass study found seasonality in $N_2O$ fluxes with higher fluxes in spring than summer or fall, suggesting some temperature dependence of $N_2O$ fluxes in seagrass ecosystems (Oreska et al. 2020). However, Camillini (2020) suggests that the $N_2O$ uptake in seagrass systems is due to denitrifiers scavenging $N_2O$ under stable oxic conditions and emission is due to variable oxic conditions stimulating incomplete nitrification.

The zero inflation of both the $CH_4$ and $N_2O$ flux data was likely caused by both sampling constraints and balanced production and consumption processes. It has been documented that GC methods for determining greenhouse gas fluxes have higher detection limits than continuous measurement methods (Brannon et al. 2016). In addition, we expect that both methane-producing and methane-consuming processes occur in the sediment and water column of this system, resulting in a measurement of net zero (Reeburgh 2007). Similarly for $N_2O$, while it is likely that some of the zero fluxes are a product of sampling constraints, zero fluxes are common and several studies have zero-inflated $N_2O$ fluxes, suggesting a balance between production and consumption processes for $N_2O$ in vegetated coastal ecosystems (Moseman-Valtierra et al. 2011; Emery and Fulweiler 2014).

### Diffusive air–sea fluxes of $CH_4$ and $N_2O$

Diffusive air–sea fluxes of $CH_4$ were similar between systems while $N_2O$ fluxes differed between systems (Table 3; Fig. 4). Both $CH_4$ and $N_2O$ were emitted across the air–sea interface and were within the range found for other seagrass-dominated systems (Table 4).

$CH_4$ emission to the atmosphere is common across marine and freshwater ecosystems due to supersaturation of the water column (Araujo et al. 2018; Rosentreter et al. 2021*b*). In Pleasant Bay, it is likely that a majority of the $CH_4$ emitted to the atmosphere is produced in the sediment. However, in East Harbor, sediment–water interface fluxes are ~ 7X lower than air–sea fluxes. Because of this, it is unlikely that the $CH_4$ emitted to the atmosphere from East Harbor is produced in the sediment or in the shallow (~ 1 m depth) water column. Potential external sources of $CH_4$ include groundwater and the surrounding saltmarsh (Sadat-Noori et al. 2016; Schutte et al. 2020). Groundwater is a significant source of $CH_4$ to the water column in some coastal bays, contributing up to 100% of $CH_4$ emissions (Sadat-Noori et al. 2016). Groundwater infiltration into coastal bays can be highly heterogeneous (Douglas et al. 2020). Because we only measured fluxes in a small area of East Harbor, we may have missed the groundwater flux. $CH_4$ can also be emitted into coastal bays by surrounding salt marshes (Schutte et al. 2020). For example, a salt marsh in coastal Georgia, USA has been shown to export 27–1200 $\mu$mol $CH_4$ $m^{-2}$ $d^{-1}$, contributing to high water column concentrations of $CH_4$ (Schutte et al. 2020). East Harbor

is bordered by a *Phragmites australis*-dominated marsh, making $CH_4$ export by the marsh a likely source of water column $CH_4$.

East Harbor also has high atmospheric concentrations of $CH_4$. High atmospheric concentrations of $CH_4$ above East Harbor may be explained by natural (e.g., ebullition) or anthropogenic (e.g., natural gas leaks, septic tank) emissions (Bastviken et al. 2004; McKain et al. 2015). East Harbor was an oligohaline to mesohaline system (4–10 ppt) from when it was diked in 1869 to more than a century later when some tidal flow was resumed in 2002 (Portnoy et al. 2006; Watts et al. 2011). Currently, East Harbor has a salinity of 20–25 ppt, but is still tidally restricted with 0.5 m tides compared to the 2.5–3.5 m tidal range in nearby systems (Portnoy et al. 2006). Thus, East Harbor may function hydrologically more like a shallow lake or pond. Ebullition from lakes and ponds can contribute up to 40–60% of system $CH_4$ emissions and are more important in shallow ecosystems, like East Harbor (Bastviken et al. 2004; Deemer and Holgerson 2021). As of 2015, there was no natural gas service to the area surrounding East Harbor (www.mass.gov). However, East Harbor is within the airshed of Boston, MA where natural gas leaks and atmospheric $CH_4$ concentrations of up to 2.6 ppm are common (McKain et al. 2015). Another potential source is off gassing from septic systems. Residential areas on the dunes surrounding East Harbor and on the southern border have septic systems (Portnoy et al. 2006). Septic systems have been shown to emit $2.9 \times 10^4$ $\mu$mol $CH_4$ capita$^{-1}$ h$^{-1}$ or 3.7 $\mu$mol $CH_4$ m$^{-2}$ h$^{-1}$ using the average lot size for Cape Cod, Massachusetts (Nowicki 1994; Diaz-Valbuena et al. 2011), making the combination of natural gas, ebullition, and septic sources of $CH_4$ likely causes of elevated atmospheric $CH_4$ concentrations above East Harbor.

In Pleasant Bay, air–sea interface $CH_4$ fluxes are 3.4X sediment–water interface fluxes. This indicates that $CH_4$ oxidation in Pleasant Bay is low and/or that there is likely another source of $CH_4$ in the basin. This source could be the natural gas deposit located in another area of the system (Borrelli et al. 2020) or it could be due to microbial $CH_4$ production in the water column (Bižić-Ionescu et al. 2018). Unlike in East Harbor, 95% of atmospheric concentrations of $CH_4$ measured in Pleasant Bay were within ±250 ppb of atmospheric concentrations during August 2019, 1863.0 ppb (https://gml.noaa.gov).

As we hypothesized, $N_2O$ was emitted to the atmosphere in both East Harbor and Pleasant Bay, with East Harbor emitting slightly more $N_2O$ than Pleasant Bay (Table 3). The only other study measuring air–sea $N_2O$ flux found uptake by a seagrass ecosystem in Wallagoot, Australia (Table 4; Camillini 2020). However, $N_2O$ emission to the atmosphere is common in nonvegetated coastal areas (Tian et al. 2020). Other coastal vegetated systems such as mangrove and tidal marshes can be sources or sinks of $N_2O$ seasonally (Murray et al. 2018; Yang et al. 2020) and across spatial gradients (Emery and Fulweiler 2017; Reading et al. 2017).

Air-sea fluxes of $N_2O$ were observed even though the mean fluxes of $N_2O$ across the sediment–water interface at both sites were zero, suggesting that the sediments were not the primary source of $N_2O$ to the atmosphere. $N_2O$ emission is often driven by DIN and oxygen concentrations via denitrification in the sediments and nitrification in the water column (Murray et al. 2015). Because the water column in the systems studied here was so shallow and well mixed, we likely captured water column processes within our incubations. Like $CH_4$, $N_2O$ can also come from external sources such as groundwater (Reading et al. 2021).

### C storage comparison

Overall, seagrass ecosystems emit less $CH_4$ and $N_2O$ than mangrove and salt marsh ecosystems ($CH_4$ median: mangrove 279.2; salt marsh 224.4; seagrass 60.6 $\mu$mol $CH_4$ m$^{-2}$ d$^{-1}$) ($N_2O$ median: mangrove 22.8; salt marsh 8.2; seagrass 0.0 $\mu$mol $N_2O$ m$^{-2}$ d$^{-1}$) (Murray et al. 2015; Al-Haj and Fulweiler 2020; Rosentreter et al. 2021*b*). Although seagrass meadows, on average, store less C than mangrove and salt marsh ecosystems (mean ± SE: 138 ± 38, 226 ± 39, 218 ± 24 g C m$^{-2}$ yr$^{-1}$, respectively) (McLeod et al. 2011), they have much lower GHG) emissions. Thus, restoration and maintenance of seagrass ecosystems may prove to be a better investment in terms of C credits per unit area than for mangrove and salt marsh ecosystems. As $CH_4$ and $N_2O$ emissions as well as C storage rates are known to be highly variable across coastal ecosystems (Rosentreter et al. 2021*a*), it is increasingly important to measure GHG fluxes in these systems to determine their true C sequestration value.

## Conclusions

Despite the mean net $CH_4$ and $N_2O$ sediment–water interface fluxes being indistinguishable from zero for nonvegetated sediments at both locations and seagrass vegetated sediments at one location, the estimated air–sea fluxes indicate that both sites were small sources of greenhouse gases to the atmosphere. These estimates suggest that there may be water column processes or inputs from other sources (e.g., groundwater) driving these results. Furthermore, while some mean fluxes were not statistically different from zero, we did measure significant individual sediment–water fluxes of $CH_4$ and $N_2O$ throughout the sampling period. Importantly, our sampling was focused on late summer months of 1 yr and thus represent a snap shot of the $CH_4$ and $N_2O$ dynamics in these temperate *Z. marina* sites. Capturing $CH_4$ and $N_2O$ fluxes over the growing season will be an important next step for determining future seagrass C budgets.

### Data availability statement

Data presented in this study can be accessed upon publication via Figshare (doi: 10.6084/m9.figshare.20079470).

## References


Al-Haj, A. N., and R. W. Fulweiler. 2020. A synthesis of methane emissions from shallow vegetated coastal ecosystems. Glob. Chang. Biol. **26**: 2988–3005. doi:10.1111/gcb.15046

Alongi, D. M., L. A. Trott, M. C. Undu, and F. Tirendi. 2008. Benthic microbial metabolism in seagrass meadows along a carbonate gradient in Sulawesi, Indonesia. Aquat Microb Ecol **51**: 141–152. doi:10.3354/ame01191

Amorocho, J., and J. J. DeVries. 1980. A new evaluation of the wind stress coefficient over water surfaces. J. Geophys. Res. Oceans **85**: 433–442. doi:10.1029/JC085IC01P00433

Aoki, L., and K. McGlathery. 2018. Restoration enhances denitrification and DNRA in subsurface sediments of Zostera marina seagrass meadows. Mar. Ecol. Prog. Ser. **602**: 87–102. doi:10.3354/meps12678

Araujo, J., A. Pratihary, R. Naik, H. Naik, and S. W. A. Naqvi. 2018. Benthic fluxes of methane along the salinity gradient of a tropical monsoonal estuary: Implications for $CH_4$ supersaturation and emission. Mar. Chem. **202**: 73–85. doi:10.1016/j.marchem.2018.03.008

Bahlmann, E., I. Weinberg, J. V. Lavrič, T. Eckhardt, W. Michaelis, R. Santos, and R. Seifert. 2015. Tidal controls on trace gas dynamics in a seagrass meadow of the Ria Formosa lagoon (southern Portugal). Biogeosciences **12**: 1683–1696. doi:10.5194/bg-12-1683-2015

Banerjee, K., A. Paneerselvam, P. Ramachandran, D. Ganguly, G. Singh, and R. Ramesh. 2018. Seagrass and macrophyte mediated $CO_2$ and $CH_4$ dynamics in shallow coastal waters. PLoS one **13**: e0203922. doi:10.1371/journal.pone.0203922

Barber, T. R. and P. R. Carlson. 1993. Effects of Seagrass Die-Off on Benthic Fluxes and Porewater Concentrations of $\Sigma CO_2$, $\Sigma H_2S$, and $CH_4$ in Florida Bay Sediments. In: Oremland, R.S. (eds) Biogeochemistry of Global Change. Springer, Boston, MA. doi:10.1007/978-1-4615-2812-8_29

Bartlett, K. B., D. S. Bartlett, R. C. Harriss, and D. I. Sebacher. 1987. Methane emissions along a salt marsh salinity gradient. Biogeochemistry **4**: 183–202. doi:10.2307/1468663

Bastviken, D., J. Cole, M. Pace, and L. Tranvik. 2004. Methane emissions from lakes: Dependence of lake characteristics, two regional assessments, and a global estimate. Global Biogeochem. Cycl. **18**: 1–12. doi:10.1029/2004GB002238

Bates, D., M. Mächler, B. Bolker, and S. Walker. 2015. Fitting Linear Mixed-Effects Models Using lme4s. J. Stat. Softw. **667**: 1–48. doi:10.18637/jss.v067.i01

Bates, D., M. Mächler, B. Bolker, and S. Walker. 2015. Fitting linear mixed-effects models using lme4. J. Stat. Softw. **67** (1): 1–48. doi:10.18637/jss.v067.i01

Bižić-Ionescu, M., D. Ionescu, M. Günthel, K. W. Tang, and H.-P. Grossart. 2018. Oxic methane cycling: New evidence for methane formation in oxic lake water. *In* A. Stams and D. Sousa [eds.], Biogenesis of hydrocarbons. Handbook of hydrocarbon and lipid microbiology. Springer. doi:10.1007/978-3-319-53114-4_10-1

Borges, A. V., J. P. Vanderborght, L. S. Schiettecatte, F. Gazeau, S. Ferrón-Smith, B. Delille, and M. Frankignoulle. 2004. Variability of the gas transfer velocity of $CO_2$ in a macrotidal estuary (the Scheldt). Estuaries **27**: 593–603. doi:10.1007/BF02907647

Borrelli, M. 2009. 137 Years of shoreline change in pleasant bay: 1868 to 2005. A report prepared for the Pleasant Bay Resource Management Alliance.

Borrelli, M., B. A. Oakley, J. B. Hubeny, H. Love, T. L. Smith, B. J. Legare, and T. Lucas. 2020. The use of multimodal data to augment shallow-water benthic habitat maps for Pleasant Bay, Cape Cod, Massachusetts: Stratigraphic data and seafloor maps. Northeast. Nat. **27**: 48–75. doi:10.1656/045.027.S1003

Bozdogan, H. 1987. Model selection and Akaike's information criterion (AIC): The general theory and its analytical extensions. Psychometrika **52**: 345–370. doi:10.1007/BF02294361

Brannon, E. Q., S. M. Moseman-Valtierra, C. W. Rella, R. M. Martin, X. Chen, and J. Tang. 2016. Evaluation of laser-based spectrometers for greenhouse gas flux measurements in coastal marshes. Limnol. Oceanogr. Methods **14**: 466–476. doi:10.1002/lom3.10105

Burkholz, C., N. Garcias-Bonet, and C. M. Duarte. 2020. Warming enhances carbon dioxide and methane fluxes from Red Sea seagrass (*Halophila stipulacea*) sediments. Biogeosciences **17**: 1717–1730. doi:10.5194/bg-17-1717-2020

Camillini, N. 2020. Carbon and nitrogen cycling in seagrass ecosystems. Southern Cross University & University of Southern Denmark.

Carini, S., N. Weston, C. Hopkinson, J. Tucker, A. Giblin, and J. Vallino. 1996. Gas exchange rates in the Parker River estuary, Massachusetts. Biol. Bull. **191**: 333–335.

Clark, J. F., P. Schlosser, H. J. Simpson, M. Stute, R. Wanninkhof, and D. T. Ho. 1995. Relationship between gas transfer velocities and wind speeds in the Tidal Hudson River determined by the dual tracer technique, p. 785–800. *In* Air–water gas transfer: Selected papers from the Third International Symposium on Air–Water Gas Transfer. AEON Verlag.

Deborde, J., and others. 2010. Methane sources, sinks and fluxes in a temperate tidal Lagoon: The Arcachon lagoon (SW France). Estuar. Coast. Shelf Sci. **89**: 256–266. doi:10.1016/j.ecss.2010.07.013

Deemer, B. R., and M. A. Holgerson. 2021. Drivers of methane flux differ between lakes and reservoirs, complicating global upscaling efforts. J. Geophys. Res. Biogeosci. **126**: e2019JG005600. doi:10.1029/2019JG005600

DeLaune, R. D., C. J. Smith, and W. H. Patrick. 1983. Methane release from Gulf coast wetlands. Tellus B **35 B**: 8–15. doi:10.1111/j.1600-0889.1983.tb00002.x

Delignette-Muller, M. L., and C. Dutang. 2015. fitdistrplus: An R package for fitting distributions. J. Stat. Softw. **64**: 1–34. doi:10.18637/jss.v064.i04

Descloux, S., V. Chanudet, D. Serça, and F. Guérin. 2017. Methane and nitrous oxide annual emissions from an old eutrophic temperate reservoir. Sci. Total Environ. **598**: 959–972. doi:10.1016/J.SCITOTENV.2017.04.066

Diaz-Valbuena, L. R., H. L. Leverenz, C. D. Cappa, G. Tchobanoglous, W. R. Horwath, and J. L. Darby. 2011. Methane, carbon dioxide, and nitrous oxide emissions from septic tank systems. Environ. Sci. Technol. **45**: 2741–2747. doi:10.1021/ES1036095

Douglas, A. R., D. Murgulet, and R. N. Peterson. 2020. Submarine groundwater discharge in an anthropogenically disturbed, semi-arid estuary. J. Hydrol. **580**: 124369. doi:10.1016/J.JHYDROL.2019.124369

Egger, M., and others. 2016. Rapid sediment accumulation results in high methane effluxes from coastal sediments. PLoS One **11**: e0161609. doi:10.1371/journal.pone.0161609

Emery, H. E., and R. W. Fulweiler. 2017. Incomplete tidal restoration may lead to persistent high CH4 emission. Ecosphere **8**: e01968. doi:10.1002/ecs2.1968

Emery, H. E., and R. W. Fulweiler. 2014. *Spartina alterniflora* and invasive *Phragmites australis* stands have similar greenhouse gas emissions in a New England marsh. Aquat. Bot. **116**: 83–92. doi:10.1016/j.aquabot.2014.01.010

Fourqurean, J. W., and others. 2012. Seagrass ecosystems as a globally significant carbon stock. Nat. Geosci. **5**: 505–509. doi:10.1038/ngeo1477

Gao, G. F., and others. 2019. *Spartina alterniflora* invasion alters soil bacterial communities and enhances soil $N_2O$ emissions by stimulating soil denitrification in mangrove wetland. Sci. Total Environ. **653**: 231–240. doi:10.1016/J.SCITOTENV.2018.10.277

Gao, Y., X. Liu, N. Yi, Y. Wang, J. Guo, Z. Zhang, and S. Yan. 2013. Estimation of $N_2$ and $N_2O$ ebullition from eutrophic water using an improved bubble trap device. Ecol. Eng. **57**: 403–412. doi:10.1016/j.ecoleng.2013.04.020

Garcias-Bonet, N., and C. M. Duarte. 2017. Methane production by seagrass ecosystems in the Red Sea. Front. Mar. Sci. **4**: 340. doi:10.3389/fmars.2017.00340

Gerard, G., and J. Chanton. 1993. Quantification of methane oxidation in the rhizosphere of emergent aquatic macrophytes: Defining upper limits. Biogeochem. **23**: 79–97. doi:10.1007/BF00000444

Grasset, C., S. Moras, A. Isidorova, R.-M. Couture, A. Linkhorst, and S. Sobek. 2021. An empirical model to predict methane production in inland water sediment from particular organic matter supply and reactivity. Limnol. Oceanogr. **9999**: lno.11905. doi:10.1002/LNO.11905

Harttung, S. A., K. R. Radabaugh, R. P. Moyer, J. M. Smoak, and L. G. Chambers. 2021. Coastal riverine wetland biogeochemistry follows soil organic matter distribution along a marsh-to-mangrove gradient (Florida, USA). Sci. Total Environ. **797**: 149056. doi:10.1016/J.SCITOTENV.2021.149056

Hothorn, T., A. Zeileis, R. W. Farebrother, C. Cummins, G. Millo, and D. Mitchell. 2020. Testing linear regression models. R package version 0.9-38.

Howes, B., S. Kelley, J. Ramsey, R. Samimy, D. Schlesinger, and E. Eichner. 2006. Massachusetts estuaries project. Linked watershed-embayment model to determine critical nitrogen loading thresholds for the Pleasant Bay System, Towns of Orleans. Massachusetts Department of Environmental Protection.

Jeffrey, L. C., G. Reithmaier, J. Z. Sippo, S. G. Johnston, D. R. Tait, Y. Harada, and D. T. Maher. 2019. Are methane emissions from mangrove stems a cryptic carbon loss pathway? Insights from a catastrophic forest mortality. New Phytol. **224**: 146–154. doi:10.1111/nph.15995

Jiang, L.-Q., W.-J. Cai, and Y. Wang. 2008. A comparative study of carbon dioxide degassing in river- and marine-dominated estuaries. Limnol. Oceanogr. **53**: 2603–2615. doi:10.4319/LO.2008.53.6.2603

Jørgensen, C. J., S. Struwe, and B. Elberling. 2012. Temporal trends in $N_2O$ flux dynamics in a Danish wetland—Effects of plant-mediated gas transport of $N_2O$ and $O_2$ following changes in water level and soil mineral-N availability. Glob. Chang. Biol. **18**: 210–222. doi:10.1111/J.1365-2486.2011.02485.X

Kim, J., S. B. Verma, and D. P. Billesbach. 1999. Seasonal variation in methane emission from a temperate Phragmites-dominated marsh: Effect of growth stage and plant-mediated transport. Glob. Chang. Biol. **5**: 433–440. doi:10.1046/j.1365-2486.1999.00237.x

Konnerup, D., J. M. Betancourt-Portela, C. Villamil, and J. P. Parra. 2014. Nitrous oxide and methane emissions from the restored mangrove ecosystem of the Ciénaga Grande de Santa Marta, Colombia. Estuar. Coast. Shelf Sci. **140**: 43–51. doi:10.1016/j.ecss.2014.01.006

Lee, K. S., F. T. Short, and D. M. Burdick. 2004. Development of a nutrient pollution indicator using the seagrass, *Zostera marina*, along nutrient gradients in three New England estuaries. Aquat. Bot. **78**: 197–216. doi:10.1016/j.aquabot.2003.09.010

Legare, B. J., O. C. Nichols, A. Mittermayr, and M. Borrelli. 2020. Relationships between species communities as determined by analysis of data from multiple surveys of Pleasant Bay, Cape Cod, MA. Northeast. Nat. **27**: 114–131. doi:10.1656/045.027.s1005

Liss, P. S., and L. Merlivat. 1986. Air–sea gas exchange rates: Introduction and synthesis. *In* P. Buat-Ménard [ed.], The role of air–sea exchange in geochemical cycling. NATO ASI Series, v. **185**. Springer. doi:10.1007/978-94-009-4738-2_5

Long, M. H., K. Sutherland, S. D. Wankel, D. J. Burdige, and R. C. Zimmerman. 2020. Ebullition of oxygen from seagrasses under supersaturated conditions. Limnol. Oceanogr. **65**: 314–324. doi:10.1002/lno.11299

Lovelock, C. E., and C. M. Duarte. 2019. Dimensions of blue carbon and emerging perspectives. Biol. Lett. **15**: 23955–26900. doi:10.1098/RSBL.2018.0781

Lyimo, L. D., M. Gullström, T. J. Lyimo, D. Deyanova, M. Dahl, M. I. Hamisi, and M. Björk. 2018. Shading and simulated grazing increase the sulphide pool and methane emission in a tropical seagrass meadow. Mar. Pollut. Bull. **134**: 89–93. doi:10.1016/j.marpolbul.2017.09.005

Macreadie, P. I., and others. 2019. The future of blue carbon science. Nat. Commun. **10**: 3998. doi:10.1038/s41467-019-11693-w

McKain, K., and others. 2015. Methane emissions from natural gas infrastructure and use in the urban region of Boston, Massachusetts. Proc. Natl. Acad. Sci. **112**: 1941–1946. doi:10.1073/PNAS.1416261112

McLeod, E., and others. 2011. A blueprint for blue carbon: Toward an improved understanding of the role of vegetated coastal habitats in sequestering $CO_2$. Front. Ecol. Environ. **9**: 552–560. doi:10.1890/110004

Moriarty, D. J. W., P. I. Boon, J. A. Hansen, W. G Hunt, I. R. Poiner, P. C. Pollard, G. W. Skyring and D. C. White. 1985. Microbial biomass and productivity in seagrass beds. Geomicrobiol. J. **4**: 21–51.

Moseman-Valtierra, S., and others. 2011. Short-term nitrogen additions can shift a coastal wetland from a sink to a source of N2O. Atmos. Environ. **45**: 4390–4397. doi:10.1016/j.atmosenv.2011.05.046

Murray, R., D. Erler, J. Rosentreter, D. Maher, and B. Eyre. 2018. A seasonal source and sink of nitrous oxide in mangroves: Insights from concentration, isotope, and isotopomer measurements. Geochim. Cosmochim. Acta **238**: 169–192. doi:10.1016/j.gca.2018.07.003

Murray, R. H., D. V. Erler, and B. D. Eyre. 2015. Nitrous oxide fluxes in estuarine environments: response to global change. Glob. Chang. Biol. **21**: 3219–3245. doi:10.1111/gcb.12923

Needelman, B. A., I. M. Emmer, S. Emmett-Mattox, S. Crooks, J. P. Megonigal, D. Myers, M. P. J. Oreska, and K. McGlathery. 2018. The science and policy of the verified carbon standard methodology for tidal wetland and seagrass restoration. Estuar. Coast. **41**: 2159–2171. doi:10.1007/s12237-018-0429-0

Neubauer, S. C., and J. P. Megonigal. 2015. Moving beyond global warming potentials to quantify the climatic role of ecosystems. Ecosystems **18**: 1000–1013. doi:10.1007/s10021-015-9879-4

Nowicki, T. P. 1994. The prospects for coastal residential development under the Cape Cod Commission Stewardship. Massachusetts Institute of Technology.

Oremland, R. S. 1975. Methane production in shallow-water, tropical marine sediments. Appl. Microbiol. **30**: 602–608. doi:10.1128/am.30.4.602-608.1975

Oreska, M. P. J., K. J. McGlathery, L. R. Aoki, A. C. Berger, P. Berg, and L. Mullins. 2020. The greenhouse gas offset potential from seagrass restoration. Sci. Rep. **10**: 1–15. doi:10.1038/s41598-020-64094-1

Orth, R. J., and others. 2006. A global crisis for seagrass ecosystems. Bioscience **56**: 987–996 doi:10.1641/0006-3568(2006)56[987:agcfse]2.0.co;2.

Poffenbarger, H. J., B. A. Needelman, and J. P. Megonigal. 2011. Salinity influence on methane emissions from tidal marshes. Wetlands **31**: 831–842. doi:10.1007/s13157-011-0197-0

Portnoy, J., S. Smith, E. Gwilliam, and K. Chapman. 2006. Annual report on estuarine restoration at East Harbor (Truro, MA), Cape Cod National Seashore, September 2006. National Park Service.

Ray, N. E., T. J. Maguire, A. N. Al-Haj, M. C. Henning, and R. W. Fulweiler. 2019. Low greenhouse gas emissions from oyster aquaculture. Environ. Sci. Technol. **53**: 9118–9127. doi:10.1021/acs.est.9b02965

Reading, M. J., I. R. Santos, D. T. Maher, L. C. Jeffrey, and D. R. Tait. 2017. Shifting nitrous oxide source/sink behaviour in a subtropical estuary revealed by automated time series observations. Estuar. Coast. Shelf Sci. **194**: 66–76. doi:10.1016/j.ecss.2017.05.017

Reading, M. J., D. R. Tait, D. T. Maher, L. C. Jeffrey, R. E. Correa, J. P. Tucker, H. A. Shishaye, and I. R. Santos. 2021. Submarine groundwater discharge drives nitrous oxide source/sink dynamics in a metropolitan estuary. Limnol. Oceanogr. **9999**: lno.11710. doi:10.1002/lno.11710

Reeburgh, W. S. 2007. Oceanic methane. Biogeochemistry **107**: 486–513. doi:10.1021/CR050362V

Rhee, T. S., A. J. Kettle, and M. O. Andreae. 2009. Methane and nitrous oxide emissions from the ocean: A reassessment using basin-wide observations in the Atlantic. J. Geophys. Res. Atmos. **114**: D12304. doi:10.1029/2008JD011662

Rosentreter, J. A., D. T. Maher, D. T. Ho, M. Call, J. G. Barr, and B. D. Eyre. 2017. Spatial and temporal variability of $CO_2$ and $CH_4$ gas transfer velocities and quantification of the $CH_4$ microbubble flux in mangrove dominated estuaries. Limnol. Oceanogr. **62**: 561–578. doi:10.1002/lno.10444

Rosentreter, J. A., D. T. Maher, D. V. Erler, R. H. Murray, and B. D. Eyre. 2018. Methane emissions partially offset "blue carbon" burial in mangroves. Sci. Adv. **4**: eaao4985. doi:10.1126/sciadv.aao4985

Rosentreter, J. A., A. N. Al-Haj, R. W. Fulweiler, and P. Williamson. 2021*a*. Methane and nitrous oxide emissions complicate coastal blue carbon assessments. Global Biogeochem. Cycl. **35**: e2020GB006858. doi:10.1029/2020GB006858

Rosentreter, J. A., and others. 2021*b*. Half of global methane emissions come from highly variable aquatic ecosystem sources. Nat. Geosci. **14**: 225–230. doi:10.1038/s41561-021-00715-2

Sadat-Noori, M., D. T. Maher, and I. R. Santos. 2016. Groundwater discharge as a source of dissolved carbon and

greenhouse gases in a subtropical estuary. Estuar. Coast. **39**: 639–656. doi:10.1007/s12237-015-0042-4

Sansone, F. J., T. M. Rust, and S. V. Smith. 1998. Methane distribution and cycling in Tomales Bay, California. Estuaries **21**: 66–77. doi:10.2307/1352547

Sargent, M. R., C. Floerchinger, K. McKain, J. Budney, E. W. Gottlieb, L. R. Hutyra, J. Rudek, and S. C. Wofsy. 2021. Majority of US urban natural gas emissions unaccounted for in inventories. Proc. Natl. Acad. Sci. USA **118**(44): e2105804118. doi:10.1073/PNAS.2105804118/SUPPL_FILE/PNAS.2105804118.SAPP.PDF

Schorn, S., and others. 2022. Diverse methylotrophic methanogenic archaea cause high methane emissions from seagrass meadows. Proc. Natl. Acad. Sci. **118**: e2106628119. doi:10.1073/PNAS.2106628119

Schutte, C. A., W. S. Moore, A. M. Wilson, and S. B. Joye. 2020. Groundwater-driven methane export reduces salt marsh blue carbon potential. Glob. Biogeochem. Cycl. **34** (10): e2020GB006587. doi:10.1029/2020GB006587

Strickland, J., and T. Parsons. 1968. A practical handbook of seawater analysis, 2nd ed. Fisheries Research Board of Canada.

Sturm, K., Z. Yuan, B. Gibbes, U. Werner, and A. Grinham. 2014. Methane and nitrous oxide sources and emissions in a subtropical freshwater reservoir, south East Queensland, Australia. Biogeosciences **11**: 5245–5258. doi:10.5194/BG-11-5245-2014

Tian, H., and others. 2020. A comprehensive quantification of global nitrous oxide sources and sinks. Nature **586**: 248–256. doi:10.1038/s41586-020-2780-0

Tokoro, T., S. Hosokawa, E. Miyoshi, K. Tada, K. Watanabe, S. Montani, H. Kayanne, and T. Kuwae. 2014. Net uptake of atmospheric $CO_2$ by coastal submerged aquatic vegetation. Global Chang. Biol. **20**: 1873–1884. doi:10.1111/gcb.12543

Trevathan-Tackett, S. M., A. C. G. Thomson, P. J. Ralph, and P. I. Macreadie. 2018. Fresh carbon inputs to seagrass sediments induce variable microbial priming responses. Sci. Total Environ. **621**: 663–669. doi:10.1016/j.scitotenv.2017.11.193

Tseng, H. C., C. T. A. Chen, A. V. Borges, T. A. DelValls, C. M. Lai, and T. Y. Chen. 2016. Distributions and sea-to-air fluxes of nitrous oxide in the South China Sea and the West Philippines Sea. Deep Sea Res. Part I Oceanogr. Res. Pap. **115**: 131–144. doi:10.1016/j.dsr.2016.06.006

Wanninkhof, R. 2014. Relationship between wind speed and gas exchange over the ocean revisited. Limnol. Oceanogr. Methods **12**: 351–362. doi:10.4319/lom.2014.12.351

Watts, I. M., J. Dean Rosati, and M. Borrelli. 2011. Re-establishing a historical inlet at East Harbor, Cape Cod, Masssachusetts. Proc. Coast. Sediments **419–429**. doi:10.1142/9789814355537_0032

Weber, T., N. A. Wiseman, and A. Kock. 2019. Global ocean methane emissions dominated by shallow coastal waters. Nat. Commun. **10**: 4584. doi:10.1038/s41467-019-12541-7

Weiss, R. F., and B. A. Price. 1980. Nitrous oxide solubility in water and seawater. Mar. Chem. **8**: 347–359. doi:10.1016/0304-4203(80)90024-9

Wiesenburg, D. A., and N. L. J. Guinasso. 1979. Equilibrium solubilities of methane, carbon monoxide, and hydrogen in water and sea water. J. Chem. Eng. Data **24**: 356–360. doi:10.1021/JE60083A006

Yang, B., X. Li, S. Lin, Z. Xie, Y. Yuan, M. Espenberg, J. Pärn, and Ü. Mander. 2020. Invasive *Spartina alterniflora* can mitigate $N_2O$ emission in coastal salt marshes. Ecol. Eng. **147**: 105758. doi:10.1016/J.ECOLENG.2020.105758

Yu, K. W., Z. P. Wang, and G. X. Chen. 1997. Nitrous oxide and methane transport through rice plants. Biol. Fertil. Soils **24**: 341–343. doi:10.1007/S003740050254

Yuan, J., D. Liu, Y. Ji, J. Xiang, Y. Lin, M. Wu, and W. Ding. 2019. *Spartina alterniflora* invasion drastically increases methane production potential by shifting methanogenesis from hydrogenotrophic to methylotrophic pathway in a coastal marsh. J. Ecol. **107**: 2436–2450. doi:10.1111/1365-2745.13164

Zeng, Y., D. A. Friess, T. V. Sarira, K. Siman, and L. P. Koh. 2021. Global potential and limits of mangrove blue carbon for climate change mitigation. Curr. Biol. **31**: 1737–1743. e3. doi:10.1016/j.cub.2021.01.070

Zheng, S., B. Wang, G. Xu, and F. Liu. 2020. Effects of organic phosphorus on methylotrophic methanogenesis in coastal lagoon sediments with seagrass (*Zostera marina*) colonization. Front. Microbiol. **11**: 1770. doi:10.3389/FMICB.2020.01770

Zhuang, G.-C., and others. 2018. Relative importance of methylotrophic methanogenesis in sediments of the Western Mediterranean Sea. Geochim. Cosmochim. Acta **224**: 171–186. doi:10.1016/J.GCA.2017.12.024

Zuur, A. F., and E. N. Ieno. 2016. Beginner's guide to zero-inflated models with R, Highland Statistics Ltd.

## Acknowledgments

Funding for this research was provided to A.N.A. by the Cape Cod National Seashore Nickerson Fellowship, Sigma Xi, Boston University Biogeosciences, the Limnology & Oceanography Research Exchange (LOREX), the Boston University Martin Luther King, Jr. Fellowship, and the Boston University Department of Earth & Environment. R.W.F. was supported by funding from Rhode Island Sea Grant and Woods Hole Sea Grant. The authors wish to acknowledge Dr. Alyssa Novak for help identifying research sites and Mr. Norval Reece and Mrs. Anne Reece for parking and beach access to one of the sites. Thanks to Brendan Kelly, Nick Ray, Claudia Mazur, Nia Bartolucci, Melissa Hagy, Cristian Triana, Gretchen McCarthy, Anniina Haka, and Ena Miculinic for field help and to John Rezza, Kwetz Mexika, Joel Sparks, and Nilotpal Ghosh for help in the lab. Thanks to Cedric Fichot for the use of their elemental analyzer.

## Conflict of interest

None declared.

*Submitted 01 October 2021*
*Revised 16 June 2022*
*Accepted 29 September 2022*

*Guest editor: David Bastviken*